Int. J. Solids Structures Vol. 20, No. 11/12, pp. 1021–1036, 1984
Printed in the U.S.A.

0020-7683/84 $3.00 + .00

FINITE DEFORMATION AND STABILITY BEHAVIOUR OF SPHERICAL INFLATABLES SUBJECTED TO AXI-SYMMETRIC HYDROSTATIC LOADING†

W. SZYSZKOWSKI AND P. G. GLOCKNER
Department of Mechanical Engineering, The University of Calgary, Calgary, Alberta, Canada

(*Received* 3 *June* 1983; *in revised form* 29 *November* 1983)

Abstract—This paper deals with the large deflection and stability behaviour of inextensible spherical air-supported membranes subjected to an accumulating ponding fluid. It is assumed that ponding fluid is available to fill an initial axi-symmetric deformation around the apex and that due to such accumulation deflections increase until under certain conditions collapse of the structure occurs.

The problem is reduced to a set of differential equations which are solved numerically to determine the parameters defining the deflected wrinkled shape of the membrane. A simple expression for use in design of such structures is obtained and the results presented in non-dimensional graphic form.

1. INTRODUCTION

This is the second in a series of three papers dealing with the axi-symmetric large deflection and stability behaviour of inextensible air supported spherical membranes subjected to axi-symmetric loading. In this paper the case of hydrostatic pressure due to an accumulating ponding medium is treated. It is assumed that an initial axi-symmetric depression around the apex is enlarged by an accumulating liquid or ponding medium which may or may not fill the depression to its capacity, depending on the density of the liquid, the internal pressure and the geometric parameters of the structure.

The wrinkled region of the membrane is considered in an Eulerian description satisfying the equations of equilibrium and the Gauss–Codazzi relation. The paper deals in detail with the case when the density of the liquid, the internal pressure and the initial geometry are such as to result in the liquid filling the axi-symmetric deformation to its capacity. This loading case is referred to as the "critical" state since no increase in load is possible. The problem is defined by a set of integro-differential equations of the Volterra type, which can be solved by a number of numerical techniques. The problem can also be stated in the form of a third-degree differential equation or, alternatively, in terms of a set of first order differential equations which are solved by a modified Euler's method, the accuracy of which is estimated to be of the order $0(1/n^2)$, where n is the number of steps used in the numerical integration. The solution technique is complicated by the fact that there are several discontinuities within the domain of integration, necessitating the division of the loaded membrane into several sub-domains (see Fig. 6). A further complication arises due to the fact that the value of the hydrostatic pressure is a function of the unknown displacement of the membrane.

Based on the results obtained, a simple approximate design expression is proposed for the large-deflection and stability behaviour of such membranes when subjected to hydrostatic pressure due to an accumulating ponding medium. The expression relates the initial imperfection or deflection, the density of the liquid and the internal pressure. The results indicate that very large structures are more sensitive to this type of loading than structures with smaller radii of curvatures.

† The results presented here were obtained in the course of research sponsored by the Natural Sciences and Engineering Research Council of Canada, Grant No. A-2736.

2. THE PROBLEM

Assume the existence of an initial axi-symmetric depression around the apex of a spherical membrane caused by an attached cable or by some imperfection. The depression is characterized by the vertical central deflection, f_0 (see Fig. 1). Assume that an accumulating ponding medium is available which can fill this depression to its capacity and/or increase the size and depth of the depression. The question arises as to what will happen to the structure under such loading conditions.

For a given internal pressure and initial geometry, the density of the ponding medium may be such that the depression will fill up to its capacity with little additional deflection taking place and the central cable remaining in tension. This, in turn, means that any further accumulation of ponding medium is impossible and that the structure will remain in stable equilibrium (see Fig. 2). On the other hand, the combination of ponding medium density, internal pressure and initial geometric parameters may be such that when a significant amount of ponding medium has accumulated in the initial depression, the tension in the cable goes to zero and the size and depth of the depression increases, without the ponding medium filling the depression to its capacity (see Fig. 3). It is assumed that ponding medium is available so as to keep on accumulating in the depression, thereby increasing the deflections and the volume and weight of the ponding medium. Clearly in such a case the structure will collapse.

These are two extreme cases. In the first case, the combination of critical parameters

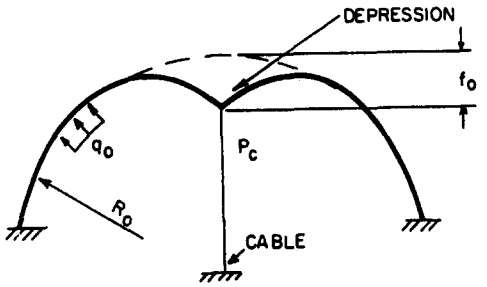

Fig. 1. Initial axi-symmetric deformation of membrane due to concentrated load.

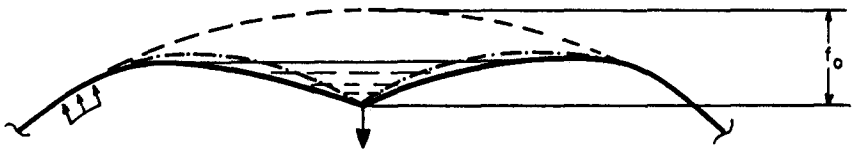

Fig. 2. Axi-symmetric deformation of membrane subjected to hydrostatic load of liquid with low density.

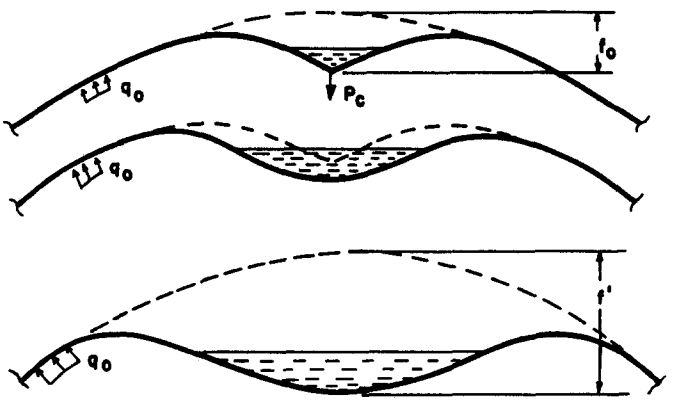

Fig. 3. Successive deflection profiles of membrane due to liquid of high density.

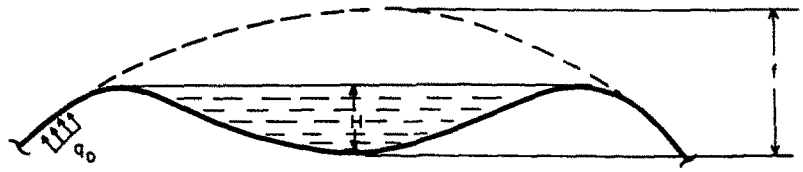

Fig. 4. Deflection profile of membrane under the action of a liquid of "critical" density.

is such that an accumulating ponding medium cannot substantially increase the size of the depression, as a result of which the structure remains stable. In the second case the combination of parameters is such that the depression grows beyond bounds and ultimately leads to collapse. There is, of course, a third possibility, namely when the density of the ponding medium, the internal pressure and the initial geometry have the right "critical" combination such that during the accumulation process there will be a loading stage reached when the ponding medium fills the depression completely and thus no further load can be applied to the structure (see Fig. 4). This paper treats this "critical" case and establishes the shape associated with this loading condition. The analysis shows that the shape associated with this "critical loading case" is independent of the pattern of the initial imperfection.

3. BASIC RELATIONSHIPS FOR AN AXI-SYMMETRICALLY WRINKLED MEMBRANE

The wrinkled region of the membrane is defined by the angle ϕ_D (see Fig. 6). In this region tensile stresses exist only in the meridional direction, while the circumferential "hoop" stress vanishes due to wrinkling. For the deformed "mean" surface of such an axi-symmetrically deformed membrane, the equations of equilibrium read

$$\frac{\mathrm{d}}{\mathrm{d}\phi}(R_\theta \sin \phi N_\phi) = 0; \quad \frac{N_\phi}{R_\phi} = q \tag{1a,b}$$

which, after simple transformations can be rearranged in the form

$$\frac{Q}{2\pi r \sin \phi} = R_\phi q; \quad Q = 2\pi \int_0^\phi q R_\phi r \cos \phi \, \mathrm{d}\phi \tag{2}$$

in which the unknown meridional membrane force, N_ϕ, was replaced by Q, representing the total force exerted on the membrane by the internal pressure; R_ϕ and R_θ denote the meridional and circumferential radii of curvatures while q is internal pressure and ϕ designates the meridional angle (see Fig. 5). For an axi-symmetrical membrane $r = R_\theta \sin \phi$ and the single (nontrivial) Gauss–Codazzi equation takes the form $R_\phi = \dfrac{1}{\cos}\dfrac{\mathrm{d}r}{\mathrm{d}\phi}$. Substituting this result into eqns (2) we have

$$\frac{\mathrm{d}r}{\mathrm{d}\phi} = \frac{Q}{2\pi r q \tan \phi}; \quad Q = 2\pi \int_0^r q r \, \mathrm{d}r \tag{3a,b}$$

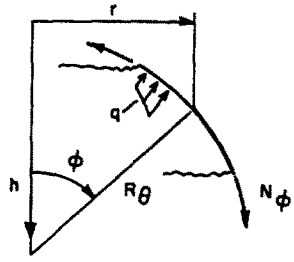

Fig. 5. Definition of coordinate system, loading and stress state.

the second of which can also be written as

$$\frac{dQ}{dr} = 2\pi rq. \tag{4}$$

If the internal pressure q is given as function of r, eqns (3) can be solved for the shape of the deformed wrinkled region in the polar coordinate system r, ϕ. To determine the shape in terms of the orthogonal coordinates (r, h), a further equation relating h to r and ϕ and given by

$$\frac{dh}{dr} = \tan \phi \tag{5}$$

has to be solved, assuming that the internal pressure is also expressed in terms of h, as

$$q = q(h) \tag{6}$$

The set of equations, eqns (3)–(6), describes any axi-symmetrically wrinkled region completely and can be solved analytically or numerically, depending on the form of the function for q.

If the material is considered to be inextensible, the solution must also satisfy the compatibility condition that the meridional arc length is unchanged during deformation.

4. EQUATIONS FOR THE WRINKLED MEMBRANE AT THE "CRITICAL" STATE

Figure 6 shows a meridional section through a spherical inextensible membrane subjected to an internal pressure, q_0, and a hydrostatic loading due to an accumulating ponding medium of density γ. The membrane is subdivided into a number of regions. In the central region, between the centre of the pond and point B, the curvature of the membrane is positive, while in the remaining outer portion, the curvature is negative.

It is quite clear that at the apex, the deformed membrane is in a stress state of all-around tension. The shape of this portion of the membrane with a biaxial stress state is spherical, as a natural consequence of the assumed inextensibility of the material. The two-way action continues out into the membrane for some distance, the spherical domain being defined by the angle ϕ_A. At that point the combination of liquid pressure, internal pressure and geometric parameters of the structure are such that the membrane starts to wrinkle in the circumferential direction. Thus at this point, designated as point A in Fig. 6, the circumferential (hoop) membrane stress changes suddenly from a positive value to zero, representing a discontinuity in the state of stress and conse-

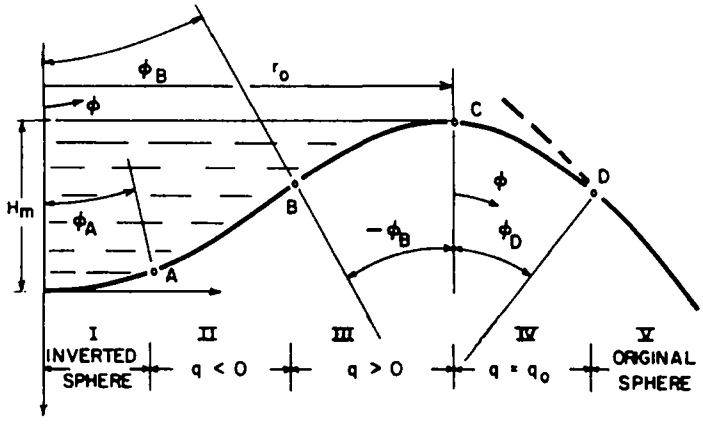

Fig. 6. Cross-section of deformed membrane in "critical" state.

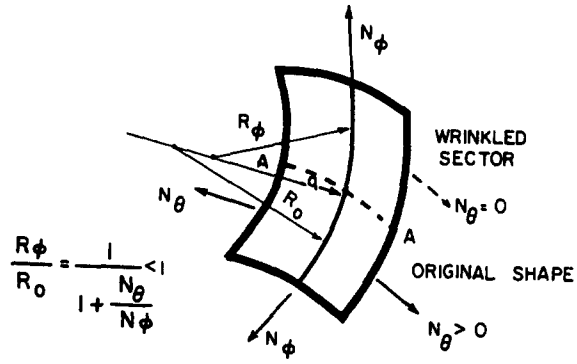

Fig. 7. Stress state at boundary between wrinkled and unwrinkled domains.

quently a discontinuity in the curvature at that point (see Fig. 7). However, the slope has to be continuous at this point, a condition which is imposed in the solution technique. A similar discontinuity in circumferential membrane stress occurs at point D, separating the wrinkled region (extending from A to D) from the outer unwrinkled spherical portion of the membrane. At points B and C, defined by ϕ_B and ϕ_D in Fig. 6, the curvatures are continuous. Due to these discontinuities, the membrane is subdivided into five regions, within each of which the hydrostatic pressure, q, and therefore the total load, Q, are analytical. Equations (3)–(6) are applied to each of these regions independently and the appropriate continuity conditions imposed at the boundaries of the regions, i.e. at points A, B, C and D.

In domains I and V, the shape of the membrane is spherical and hence

$$r = R_0 \sin \phi \text{ for } 0 \leq \phi \leq \phi_A \text{ or } \phi \geq \phi_D.$$

In domains II and III the pressure q and the total force Q are expressed as

$$q = q_0 - \gamma \left(H_m + k \int_0^r \tan \phi \, dr \right) \tag{7}$$

$$Q = \pi r^2 q_0 - \gamma \left[V_A - k \int_{r_A}^r \pi r^2 \tan \phi \, dr + \pi r^2 \left(H_m + k \int_0^r \tan \phi \, dr \right) \right] \tag{8}$$

where

$$V_A = \frac{\pi}{3} R_0^3 (1 - \cos \phi_A)(2 - \cos \phi_A - \cos^2 \phi_A)$$

$$k = \begin{cases} -1 \text{ for } \phi_A < \phi < \phi_B \\ 1 \quad \text{for } -\phi_B < \phi < 0. \end{cases}$$

Finally, in domain IV ($0 < \phi < \phi_D$) the pressure and total load are defined by

$$q = q_0$$

$$Q = \pi r^2 q_0 - \gamma \left[V_A + \int_{r_a}^{r_c} \pi r^2 \tan \phi \, dr \right]. \tag{9a}$$

As stated above, at points A and D, the boundaries between wrinkled and unwrinkled domains, continuity of slope is imposed, whereas at points B and C, the curvature must be continuous. Therefore the boundary/continuity conditions between the various domains (see Fig. 6) are established as

at point A

$$\phi_I(\phi_A^-) = \phi_{II}(\phi_A^+) \tag{10a}$$

$$r_I(\phi_A) = r_{II}(\phi_A) \rightarrow r_{II}(\phi_A) = R_0 \sin \phi_A \tag{10b}$$

at point B $$r_{II}(\phi_B) = r_{III}(-\phi_B) \tag{11}$$

$$\frac{dr_{III}}{d\phi} q_{II}\bigg|_{\phi \to \phi_B} = \frac{dr_{III}}{d\phi} q_{III}\bigg|_{\phi \to -\phi_B} \tag{12}$$

at point C $$r_{III}(0) = r_{IV}(0) \tag{13}$$

$$\frac{dr_{III}}{d\phi}\bigg|_{\phi=0} = \frac{dr_{IV}}{d\phi}\bigg|_{\phi=0} \tag{14}$$

at point D $$r_{IV}(\phi_D) = R_0 \sin \phi_D. \tag{15}$$

In domain *IV*, the outermost wrinkled region, the shape of the membrane can be determined analytically since eqn (3) takes the simple form

$$\frac{dr}{d\phi} = \frac{\pi r^2 q_0 - V_m \cdot \gamma}{2\pi r q_0 \tan \phi} \tag{16}$$

where

$$V_m = V_a + k \int_{r_A}^{r_0} \pi r^2 \tan \phi \, dr$$

denotes the entire volume of the accumulated ponding medium. The solution to eqn (16) is given as

$$r = \sqrt{\frac{1}{\pi q_0} (\gamma V_m + C \sin \phi)}$$

which after satisfying conditions (13) and (15) is rewritten as

$$r = r_0 \sqrt{1 + \left[\frac{\sin^2 \phi_D}{(r_0/R_0)^2} - 1\right] \frac{\sin \phi}{\sin \phi_D}} \tag{17}$$

where

$$r_0 = \sqrt{\frac{V_m \cdot \gamma}{\pi q_0}} = r_{III}(0) = r_{IV}(0).$$

The meridional radius of curvature, R_ϕ, is therefore obtained in the form

$$R_\phi = \frac{1}{\cos \phi} \frac{dr}{d\phi} = \frac{B \cdot r_0}{2\sqrt{1 + B \sin \phi}} \tag{18}$$

where

$$B = \left[\frac{\sin^2 \phi_D}{(r_0/R_0)^2} - 1\right] \frac{1}{\sin \phi_D}.$$

Consequently, the boundary conditions at point C may be expressed in terms of two parameters r_0 (or V_m) and ϕ_D as

$$r_{III}(0) = r_0 \tag{19a}$$

$$\frac{dr_{III}}{d\phi}\bigg|_{\phi=0} = \frac{B r_0}{2}. \tag{19b}$$

In domains *II* and *III*, eqns (3), (5) and (6) can be solved numerically only. Substituting eqns (7) and (8) into eqns (3) and (6), one obtains

$$\frac{dr}{d\phi} = \frac{\pi r^2 q_0 - \left[V_A - k\int_{r_A}^{r} \pi r^2 \tan\phi\, d\phi + \pi r^2\left(H_m + k\int_0^r \tan\phi\, dr\right)\right]}{2\pi r \tan\phi \cdot q} \tag{20}$$

$$\frac{dh}{dr} = k\tan\phi \tag{21}$$

$$q = q_0 - \gamma\left(H_m + k\int_0^r \tan\phi\, dr\right) \tag{22}$$

which is a set of integro-differential equations of the Volterra type to be solved by any one of a number of numerical methods. Alternatively, this set can be transformed into a third degree differential equation, with respect to $r(\phi)$ as

$$\frac{d}{d\phi}\left[\frac{r\tan^2\phi\left(\frac{dr}{d\phi}\right)^2}{\frac{d}{dr}\left(r\tan\phi\frac{dr}{d\phi} - r\frac{dr}{d\phi}\right)}\right] + \tan\phi\frac{dr}{d\phi} = 0. \tag{23}$$

There are difficulties with establishing boundary conditions for this equation as well as with convergence when a numerical solution is attempted. For this reason the problem was recast in the form of a set of first order differential equations. First, the dimensionless quantities

$$\bar{r} = r/R_0, \quad \bar{h} = h/R_0, \quad \bar{V} = V/\pi R_0^3$$

$$\bar{q} = q/q_0, \quad \bar{Q} = Q/\pi R_0^2 q_0, \quad \bar{\gamma} = R_0\gamma/q_0$$

are introduced into eqns (20)–(22) after which one obtains

$$\frac{d\bar{r}}{d\phi} = \frac{\bar{r}^2\bar{q} - \bar{V}\bar{\gamma}}{2\bar{r}\bar{q}\tan\phi}$$

$$\frac{d\bar{h}}{d\bar{r}} = k\tan\phi$$

where

$$\bar{q} = 1 - (\bar{H}_m + \bar{h})\bar{\gamma} \tag{24}$$

$$\bar{V} = \bar{V}_A - \int_{r_A}^{\bar{r}} \bar{r}^2\, d\bar{h}.$$

From eqn (24) one obtains

$$\frac{d\bar{V}}{d\bar{h}} = -\bar{r}^2.$$

Finally, instead of eqns (20)–(22), we arrive at the simple set of equations

$$\frac{d\bar{r}}{d\phi} = \frac{\bar{r}^2\bar{q} - \bar{V}\bar{\gamma}}{2\bar{r}\bar{q}\tan\phi} \tag{26a}$$

$$\frac{d\bar{h}}{dr} = k\tan\phi \tag{26b}$$

$$\frac{d\bar{V}}{d\bar{h}} = -\bar{r}^2 \tag{26c}$$

$$\bar{q} = 1 - (\bar{H}_m + \bar{h})\bar{\gamma}. \tag{26d}$$

Since the boundary conditions, eqns (10) and (19), depend on ϕ_A, ϕ_D and r_0, the shape of the wrinkled membrane in domains *II* and *III* can be determined as a function of these quantities.

Finally, the inextensibility condition has to be met which imposes the condition

$$\int_{\bar{r}_A\bar{r}_A}^{\bar{r}_D\bar{r}_D} \frac{d\bar{r}}{\cos\phi} = \phi_D - \phi_A. \tag{27}$$

5. NUMERICAL SOLUTION TECHNIQUE

The set of equations, eqns (26), were solved using a modified Euler's method, the accuracy of which is estimated to be of the order $0(1/n^2)$, where n is the number of steps used in the numerical integration process. The procedure was carried out as follows:

(1) Assume an increment for $\Delta\phi$, and assume that values for all parameters are known at point i. Therefore one can obtain

$$\Delta\bar{r}_i' = f_i\Delta\phi \quad \text{where} \quad f_i = \frac{\bar{r}^2\bar{q} - \bar{V}\bar{\gamma}}{2\bar{r}\bar{q}\tan\phi} \tag{28a}$$

$$\Delta\bar{h}_i' = k\tan\phi_i\Delta\bar{r}_i' \tag{28b}$$

$$\Delta\bar{V}_i' = \bar{r}_i'^2\Delta\bar{h}_i' \tag{28c}$$

and

$$\phi_{i+1}' = \phi_i + \Delta\phi; \quad \bar{r}_{i+1}' = \bar{r}_i' + \Delta\bar{r}_i'; \quad \bar{h}_{i+1}' = \bar{h}_i + \Delta\bar{h}_i'; \quad \bar{V}_{i+1}' = \bar{V}_i + \Delta\bar{V}_i$$

where the primed quantities are intermediate values used in obtaining increments for the parameters corresponding to the next point.

(2) Increments of the respective functions are calculated by means of the expressions

$$\Delta\bar{r}_i = \frac{1}{2}(f_i + f_{i+1})\Delta\phi \tag{29a}$$

$$\Delta\bar{h}_i = \frac{k}{2}(\tan\phi_i + \tan\phi_{i+1}')\Delta\bar{r}_i \tag{29b}$$

$$\Delta\bar{V}_i = -\frac{1}{2}(\bar{r}_i^2 + \bar{r}_{i+1}'^2)\Delta\bar{h}_i \tag{29c}$$

and finally

$$\phi_{i+1} = \phi_i + \Delta\phi; \quad \bar{r}_{i+1} = \bar{r}_i + \Delta\bar{r}_i; \quad \bar{h}_{i+1} = \bar{h}_i + \Delta\bar{h}_i; \quad \bar{V}_{i+1} = \bar{V}_i + \Delta\bar{V}_i.$$

The procedure is initiated by assuming values for the non-dimensional liquid depth at the axis of symmetry, $\bar{H}_m$, the non-dimensional density $\bar{\gamma}$, and the angle ϕ_A denoting the location of point A. Since the shape of the membrane is known in the unwrinkled central spherical region (between points 0 and A) the actual numerical integration starts at point A in accordance with the above outlined procedure, using the preselected value of $\Delta\phi$. The procedure is continued until the nondimensional pressure $\bar{q} = 0$ which corresponds to point B (Fig. 6), the inflection point along the deflected membrane. At

this location, values of the parameter k and ϕ have to be altered, namely k has to be changed from -1 to 1, and ϕ_B has to be changed to $-\phi_B$.

The procedure is continued until point C ($\phi = 0$) is reached where the actual value of $\bar{q}$ is verified. Naturally this value should be equal to 1. If $\bar{q}_c < 1$, the assumed density is not large enough to keep the membrane in equilibrium with the internal pressure q_0 and therefore must be increased in accordance with the expression

$$\bar{\gamma}_{j+1} = \bar{\gamma}_j/\bar{q}_j(0). \tag{30}$$

The whole process is repeated until the required accuracy defined by

$$|\bar{q}_j(0) - 1| < \epsilon \tag{31}$$

is obtained, where ϵ is any preselected small positive number.

Using this procedure with an assumed value for the nondimensional liquid depth and a value for ϕ_A, the corresponding value for the nondimensional density of the accumulation ponding medium can be determined.

Next the continuity conditions, eqns (19), are considered at point C. The radius of curvature at this point can be written in the form

$$\left.\frac{d\bar{r}}{d\phi}\right|_{\phi=0} = g_0 = \bar{r}_c\left(\frac{\sin^2\phi_D}{\bar{r}_c^2} - 1\right)/(2\sin\phi_D) \tag{32}$$

where $g_0 = g(0)$ and $\bar{r}_c$ are known from the numerical integration process (eqns 28 and 29). The position of point D is determined from eqn (32) since

$$\sin\phi_D = \bar{r}_c(g_0 + \sqrt{1 + g_0}). \tag{33}$$

The shape of the wrinkled membrane in domain *IV* is found using eqn (17) which, of course, corresponds to the assumed value of $\bar{H}_m$ and is a function of the angle ϕ_A. To establish the value of ψ_A the inextensibility condition, eqn (27), is imposed by

$$S(\phi_A) = \phi_D - \phi_A \tag{34}$$

where

$$S(\phi_A) = \int_{\bar{r}_A}^{\bar{r}_D} \frac{d\bar{r}}{\cos\phi}$$

denotes the dimensionless length of the deformed arc which is calculated numerically during the integration process. On the basis of eqn (34) the value of ϕ_A is established as

$$\phi_A^{(n+1)} = \phi_D^{(n)} - S(\phi_A^{(n)})$$

where $\phi_D^{(n)}$ is obtained from eqn (33) for an assumed value $\phi_A^{(n)}$. The procedure is repeated until the required accuracy defined by

$$\left|\frac{\phi_A^{(n+1)} - \phi_A^{(n)}}{\phi_A^{(n)}}\right| \leq \epsilon \tag{36}$$

is reached, where ϵ is an arbitrarily chosen small positive constant. For an assumed value of the nondimensional liquid depth, $\bar{H}_m$, the critical shape of the deformed wrinkled membrane is completely determined by this procedure and the corresponding nondimensional density, $\bar{\gamma}$, and all parameters of deformation are established.

6. NUMERICAL RESULTS

The equations defining the problem have been numerically integrated by the above described procedure for a range of values of the nondimensional liquid depth at the axis of symmetry, $\overline{H}_m$. On Fig. 8 the results of this analysis are shown in graphical form, where the parameters of deformation, ϕ_A, ϕ_B, ϕ_D, the dimensionless density, $\overline{\gamma}$, and the dimensionless weight of the liquid, $\overline{P}$, are plotted as functions of $\overline{H}_m$.

It was established that as $\overline{H}_m \to 0.801$ the angle $\phi_D \to 86.4°$ and the numerical procedure becomes divergent. This, in turn, means that for $\overline{H}_m \geq 0.801$ the state of equilibrium for the "critical" shape of the deformed membrane (see Fig. 4) does not exist.

Figure 9 gives a cross-section of half the membrane for various values of assumed non-dimensional liquid depth at the axis of symmetry. In Fig. 10 the key parameters, including $\bar{r}$, $\overline{V}$, $\overline{H}_m$, and the inverse of the non-dimensional density, $\overline{\gamma}^{-1} = q_0/R_0\gamma$ are plotted as a function of the total nondimensional vertical displacement $\overline{f} = f/R_0$ at the axis of symmetry. There are two things which are noteworthy on this diagram. Firstly, the total central deflection and the nondimensional liquid depth at the axis of symmetry are proportional, as is shown by the lowest of the lines in Fig. 10. What is perhaps more surprising, and fortuitous, is the fact that the nondimensional inverse density can also be approximated by a straight line given by

$$\overline{\gamma}^{-1} = \frac{q_0}{\gamma R_0} \cong 0.212\,\frac{f}{R_0} = 0.212\,\overline{f} \tag{37}$$

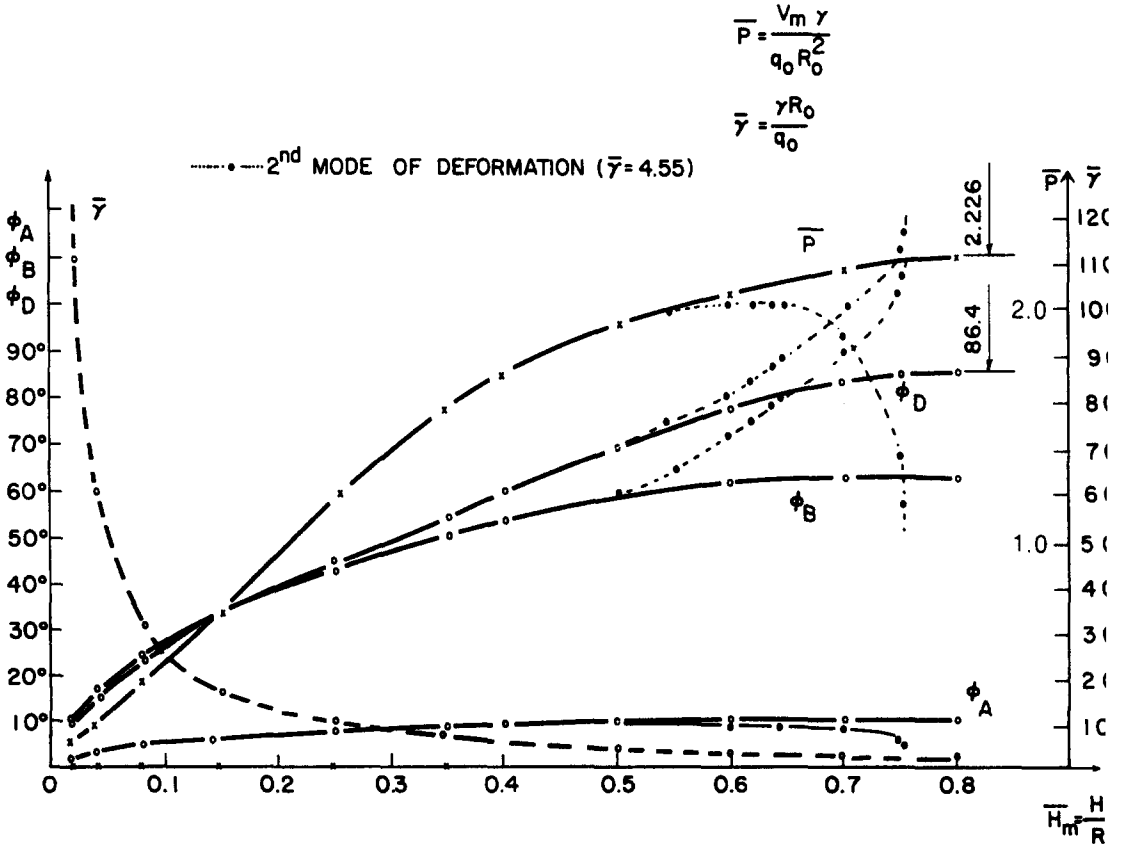

Fig. 8. Plot of key parameters vs non-dimensional liquid depth.

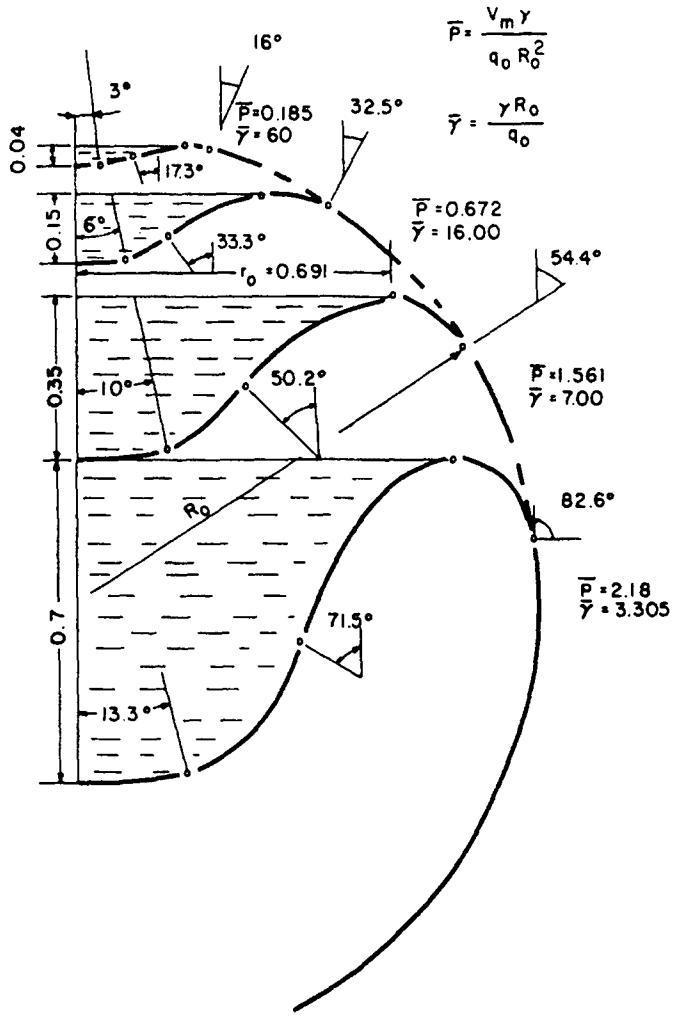

Fig. 9. Deflection profiles for various liquid densities.

on the basis of which we arrive at the following very simple design expression relating the three critical design parameters

$$\frac{q_0}{\gamma \cdot f} = 0.212. \tag{38}$$

This expression permits an estimation of the initial allowable axisymmetric depression around the apex of a spherical inflatable for a given ponding medium before accumulation of that medium in the depression leads to catastrophic results. For example, if we assume that the internal overpressure is 400 Pa, then the maximum initial central deflection at the apex, f_{cr}, is estimated as

$$f_{cr} = \frac{400}{0.212 \cdot 9810} = 0.192 \text{ m}.$$

What is perhaps surprising is the fact that the magnitude of this initial central deflection or imperfection does not depend on the initial radius R_0 of the membrane. Since the maximum stress in the membrane is a direct function of R_0, which implies that the larger the membrane the smaller the internal pressure, and therefore this result shows that spherical structures with large radii of curvatures are more sensitive to imperfec-

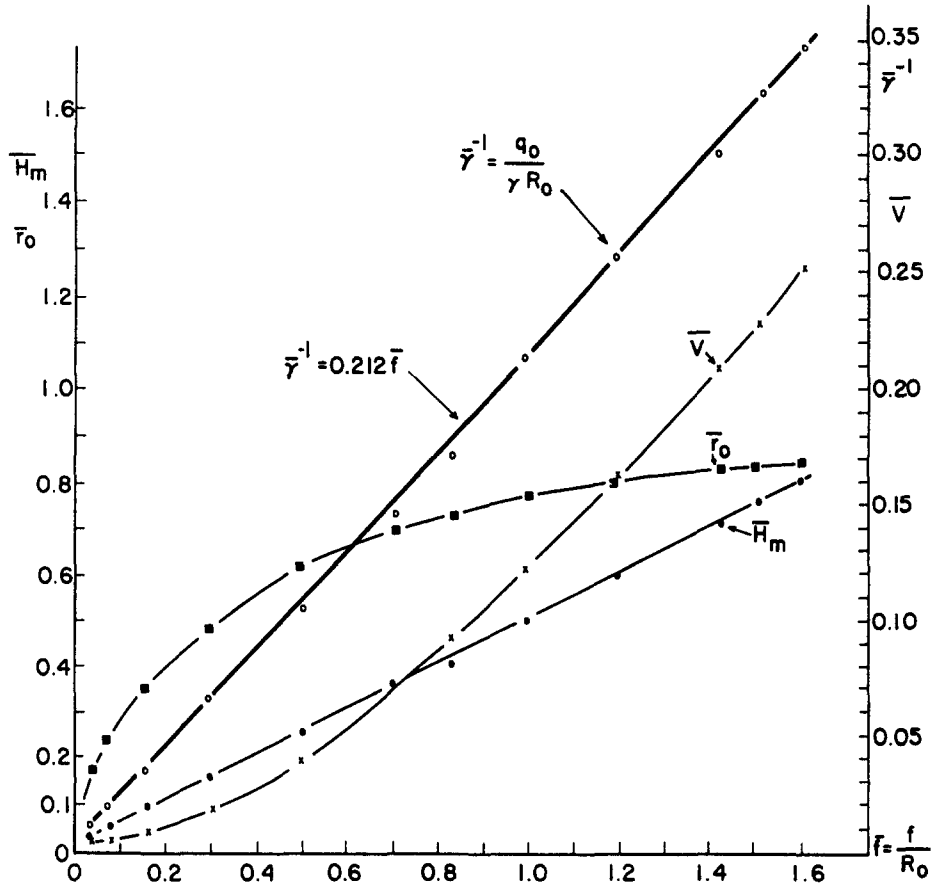

Fig. 10. Plot of key parameters vs total deflection.

tions and initial inward deflections than structures with sharper radii of curvatures; i.e. collapse due to an accumulation of ponding medium resulting from an initial depression around the apex of the structure is more likely for a structure with a very large radius.

The total weight of the accumulating ponding medium is plotted against nondimensionalized deflection at the axis of symmetry in Fig. 11 by means of the heavy curve. For comparison purposes the graph for a concentrated load applied at the apex is also shown (see [1]). An approximate solution in the relatively small deflection domain, based on an energy method and assumed isometric deformations [2] is indicated by a straight line tangential to the initial portion of the curve for liquid loading.

Although the overall shape of the two curves shown in Fig. 11 are similar in appearance, their physical meaning is quite different. In the case of the liquid loading, each point on the curve corresponds to the "critical state" of loading and represents a value of the nondimensional liquid density corresponding to that critical state. For example if $\bar{f}$ is approx. 0.7, the critical dimensionless density equals 7.0 and the total dimensionless weight of the liquid $\bar{P} \cong 1.57$. As can be seen from this graph the maximum weight of accumulating ponding medium $\bar{P}_{max} = 2.226$ which corresponds to the minimum dimensionless density $\bar{\gamma}_{min} = 2.86$. This density, in turn, implies that if $\bar{\gamma} < 2.86$, a "critical state," as indicated in Fig. 4, is impossible, since the internal pressure will be high enough so as to keep the initial depression from growing, irrespective of its initial magnidude. A spherical inflatable may therefore be classified as "absolutely stable" under a hydrostatic loading due to an accumulating ponding medium, provided the following condition is satisfied

$$\frac{\gamma R_0}{q_0} \leq 2.86. \tag{39}$$

The practical significance of this expression may be rather limited since for an internal pressure $q_0 = 400$ Pa and density of water $\gamma = 9810$ N/m^3, the radius for such an "absolutely safe" spherical inflatable is calculated as less than 0.117 m.

Due to the similarity of the load-deflection diagram of the liquid loading and concentrated loading, shown in Fig. 11, and because the load deflection diagram for the concentrated load shows stable and unstable regions (see [1]), attempts were made to obtain results for the liquid loading case which correspond to the "second" and "third" modes of failure; i.e. the unstable region and the case of the entirely wrinkled membrane. For the mode of deformation indicated in Fig. 6, the numerical procedure proved to be divergent for nondimensional deflections $\bar{f} \gtrsim 1.72$ (or $\bar{H}_m > 0.801$). For this reason, the second mode of deformation, indicated in Fig. 12, was analyzed in which the accumulating ponding medium does not fill the depression to its capacity. The governing equations are identical to those used for the critical case. The boundary conditions are also similar, but now point C, the point where the pressure due to the ponding medium is 0, is unknown and must be determined for a given density. The

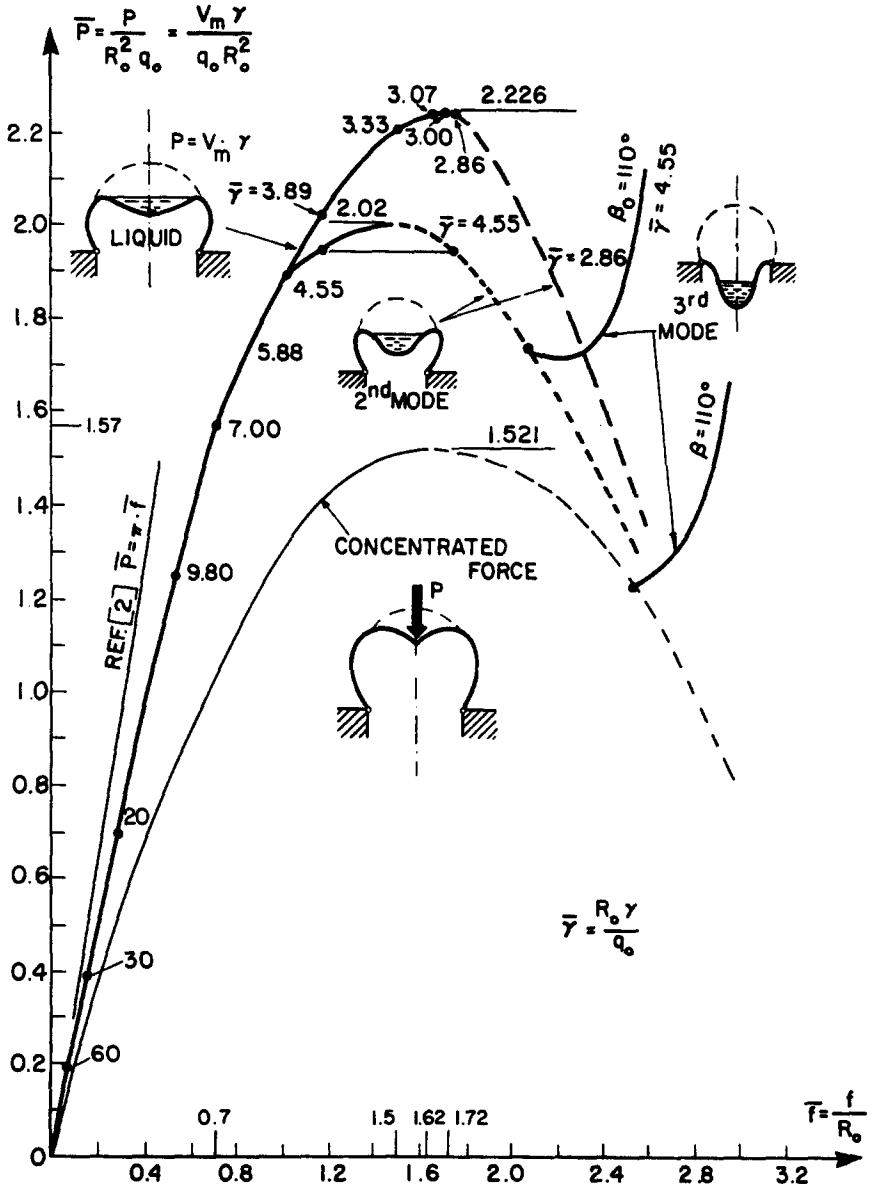

Fig. 11. Non-dimensional load-deflection curves.

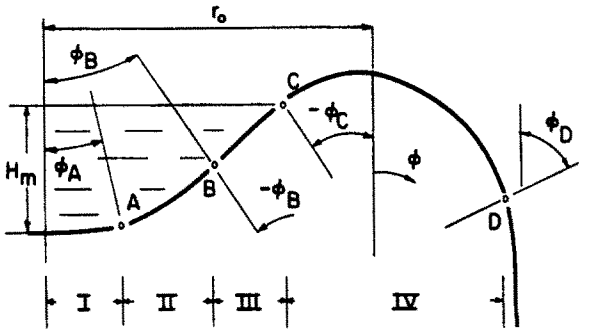

Fig. 12. Deflection profile for liquid loading with density greater than "critical" value.

numerical procedure is similar to that used above. One starts at point A and assumes the values of the nondimensional liquid depth, $\bar{H}_m$, the nondimensional density $\bar{\gamma}$, and the angle ϕ_A. Next the integration process, using eqns (28) and (29), is continued until $\bar{q} = 1$, which corresponds to point C on the deflected membrane; thus $\bar{r}_c$ and ϕ_c are determined. If $\phi_c \geq 0$, a larger nondimensional density value $\bar{\gamma}$ must be assumed. Next the values of ϕ_D and $\bar{r}_0$ are calculated using the boundary condition at point C and the relations (17) and (18)

$$B = \frac{1}{\dfrac{\bar{r}_c}{2\bar{R}_\phi} - \sin\phi_c}$$

$$\bar{r}_0 = \frac{\bar{r}_c}{\sqrt{1 + B\sin\phi_c}} \tag{40}$$

$$\sin\phi_D = \frac{B\bar{r}_0^2}{2}\left(1 + \sqrt{1 + \frac{4}{B^2\bar{r}_0^2}}\right)$$

where

$$\bar{R}_\phi = \frac{1}{\cos\phi_c}\frac{d\bar{r}}{d\phi}\bigg|_c.$$

Finally the inextensibility condition, eqn (34), is used to solve for ϕ_A to within a predetermined accuracy as defined by eqn (36).

This procedure was applied for a single value of the dimensionless density $\bar{\gamma} = 4.55$. Two solutions, corresponding to two possible equilibrium states, were established and

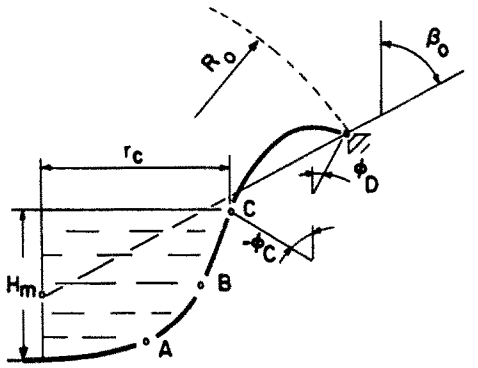

Fig. 13. Deflection profile of completely wrinkled membrane.

the corresponding deformation parameters and load are indicated in Fig. 8. Figure 11 also indicates the "second mode behaviour" for a nondimensional density $\bar{\gamma} = 4.55$. From this result and an analogy with the "second mode behaviour" for the case of the axi-symmetric concentrated load, we conclude that the first or so-called "critical state," in which the ponding medium fills the depression to capacity, corresponds to stable equilibrium and implies values for $\phi_D < 90°$.

Finally the case of the entirely wrinkled membrane, supported along its perimeter and subjected to a hydrostatic loading resulting from an accumulating ponding medium, was analyzed (see Fig. 13). The numerical procedure is identical to that used for an investigation of the "second mode type" behaviour. Only the boundary condition has to be modified to read

$$r_{IV}(\phi_D) = R_0 \sin \beta_0.$$

Relations (40) must also be slightly changed. From the continuity condition at point C one obtains

$$B = \frac{1}{\dfrac{\bar{r}_c}{2\bar{R}_\phi} - \sin \phi_c} \tag{41a}$$

$$\bar{r}_0 = \frac{\bar{r}_c}{\sqrt{1 + B \sin \phi_c}} \tag{41b}$$

$$\sin \phi_D = \left(\frac{\sin^2 \beta_0}{\bar{r}_0^2} - 1\right) / B \tag{41c}$$

which, together with the inextensibility condition, eqn (34), and assumed values for $\bar{H}_m$ and $\bar{\gamma}$ leads to a determination of all load and deformation parameters. This "third mode of failure" was solved for only a single nondimensional density case $\bar{\gamma} = 4.55$. The result is shown in the top right area of Fig. 11. By analogy with the case of the axi-symmetric concentrated load, and for obvious physical reasoning, this mode of deformation and the associated equilibrium must be stable.

7. CONCLUSIONS

The large deformation and stability behaviour of inextensible spherical inflatables subjected to internal pressure and axi-symmetric hydrostatic loading resulting from an accumulating ponding medium has been investigated. It is shown that for such structures the possibility of increasing deflections and ultimate collapse due to an accumulating ponding medium is possible provided

$$\frac{\gamma R_0}{q_0} > 2.86.$$

A relation between critical values of the internal pressure and density of the liquid and the allowable maximum deflection or initial imperfection at the apex are related by an approximate expression given as

$$\frac{q_0}{\gamma f} \cong 0.212.$$

Since stress and strength considerations for the membrane will impose a smaller internal pressure for structures with large radii of curvatures, this expression implies that for a given density, like that of water, the allowable imperfections or initial depressions are smaller the larger the radius of curvature of the structure. This, in turn, implies

that large air-supported spherical membranes are more sensitive to collapse by an accumulating ponding medium, initiated by initial imperfections, than are structures with smaller dimensions.

Air supported membranes generally exhibit features in their large deflection and stability behaviour which are very similar to and are characteristic of the stability behaviour of elastic shells [1]. Since shells as a rule are highly imperfection sensitive, by analogy one might expect that air supported membranes behave in a similar manner. Indeed, in a recent study [3], the imperfection sensitivity of such inflatables was confirmed experimentally, since the critical values obtained by experiments were consistently lower than the corresponding theoretical predictions. It may therefore be important to verify the above conclusions by means of carefully planned and executed experiments before the approximate expression suggested in this paper is adopted for codes or is used in the design of large-scale inflatable structures.

REFERENCES

1. S. Szyszkowski and P. G. Glockner, Finite deformation and stability behaviour of spherical inflatables under axi-symmetric concentrated loads. *Int. J. Non-Linear Mechanics* **19**,(5) 489–496 (1984).
2. S. Lukasiewicz and P. G. Glockner, Collapse by ponding of shells. *Int. J. Solids Structures* **19**, 251–261 (1983).
3. D. J. Malcolm and P. G. Glockner, Collapse by ponding of air-supported membranes. *J. Structural Div.*, 1525–1532 (1978).